AIP | Review of Scientific Instruments

A cryogen-free dilution refrigerator based Josephson qubit measurement system

Ye Tian, H. F. Yu, H. Deng, G. M. Xue, D. T. Liu, Y. F. Ren, G. H. Chen, D. N. Zheng, X. N. Jing, Li Lu, S. P. Zhao, and Siyuan Han

Citation: Review of Scientific Instruments **83**, 033907 (2012); doi: 10.1063/1.3698001

View online: http://dx.doi.org/10.1063/1.3698001

View Table of Contents: http://scitation.aip.org/content/aip/journal/rsi/83/3?ver=pdfcov

Published by the AIP Publishing

A cryogen-free dilution refrigerator based Josephson qubit measurement system

Ye Tian,[1] H. F. Yu,[1] H. Deng,[1] G. M. Xue,[1] D. T. Liu,[1] Y. F. Ren,[1] G. H. Chen,[1] D. N. Zheng,[1] X. N. Jing,[1] Li Lu,[1] S. P. Zhao,[1] and Siyuan Han[2]
[1]*Beijing National Laboratory for Condensed Matter Physics, Institute of Physics, Chinese Academy of Sciences, Beijing 100190, China*
[2]*Department of Physics and Astronomy, University of Kansas, Lawrence, Kansas 66045, USA*

(Received 14 January 2012; accepted 9 March 2012; published online 30 March 2012)

We develop a small-signal measurement system on cryogen-free dilution refrigerator which is suitable for superconducting qubit studies. Cryogen-free refrigerators have several advantages such as less manpower for system operation and large sample space for experiment, but concern remains about whether the noise introduced by the coldhead can be made sufficiently low. In this work, we demonstrate some effective approaches of acoustic isolation to reduce the noise impact. The electronic circuit that includes the current, voltage, and microwave lines for qubit coherent state measurement is described. For the current and voltage lines designed to have a low pass of dc-100 kHz, we show that the measurements of Josephson junction's switching current distribution with a width down to 1 nA, and quantum coherent Rabi oscillation and Ramsey interference of the superconducting qubit can be successfully performed. © *2012 American Institute of Physics*. [http://dx.doi.org/10.1063/1.3698001]

I. INTRODUCTION

Experimental studies of superconducting qubits require mK temperature environment with extremely low electromagnetic (EM) noise level, so that coherent quantum states of qubits can be prepared, maintained, and controlled and their delicate coherent evolution can be monitored and measured.[1–4] So far, most of these experiments are performed using dilution refrigerators that use liquid He^4 as cryogen for the first-stage cooling. However, for such traditional wet systems, there are several obvious disadvantages. For instance, even "low-loss" Dewars require refilling every few days, therefore it is not only more expensive but also requires more manpower, infrastructure, and time to conduct experiments. Also, the need for a narrow neck in the helium Dewar to keep the boil-off to an acceptable level means that the space available for experimental wiring and other experimental services is limited. Moreover, the cold vacuum seal also means hermetically sealed and cryogenically compatible wiring feedthroughs are required in addition to the room temperature fittings.

There has been much recent interest in the dry dilution refrigerators which use pulse-tube coolers to provide the first-stage cooling instead of the liquid cryogen. For these dry systems, the above mentioned disadvantages are avoided. Namely, they need much less manpower to operate and have a much larger sample space. The smaller overall size of the systems is also convenient for magnetic shielding and other lab-space arrangements. In addition, they do not rely on liquid He^4 cryogen which is becoming a more expensive natural resource.

Presently, there are still less users for the dry system than those for the wet system. A main concern about using pulse-tube based dilution refrigerators for sensitive small signal measurements is whether noises (vibration, electrical, and acoustic) introduced by the coldhead is sufficiently low. In this paper, we describe the design, construction, and characterization of a system built on an Oxford DR200 cryogen-free dilution refrigerator suitable for experiments that are extremely sensitive to their electromagnetic environments. The paper is organized as follows. We first describe the mechanical constructions which reduce the acoustic vibrations to a very low level. We then present the electronic measurement setup that includes various filtering, attenuation, and amplification for different parts of the qubit quantum state preparation and measurement. Finally, we show that the system is adequate for studying coherent quantum dynamics of superconducting qubits by demonstrating Rabi oscillation and Ramsey fringe in an Al superconducting phase qubit.

II. MECHANICAL CONSTRUCTION

Figure 1(a) shows the front view of our system with the DR200 refrigerator installed on an aluminum-alloy frame near the center. The refrigerator can reach its base temperature of 8 mK and temperatures below 20 mK, respectively, before and after all electronic components and measurement lines described below are installed. It has a prolonged version compared to the Oxford's standard design and has a large sample space of 25 cm in diameter and 28 cm in height. To reduce vibrations coupled from the floor, the aluminum-alloy frame is placed on four 0.8 cm thick rubber stands. The refrigerator can be attached to the frame via an air-spring system to provide further vibration isolation. The turbo pump, originally placed on the top of the refrigerator, is moved to the other side of the wall in the next room and is connected to the fridge by a stainless steel pipe and a 1 m long bellows as can be seen in Fig. 1(b). Both the pipe and the bellows have the same diameter as that of the inlet of the turbo pump. This setup proves significantly reducing the vibrations from the turbo pump. Furthermore, the rotary valve is separated

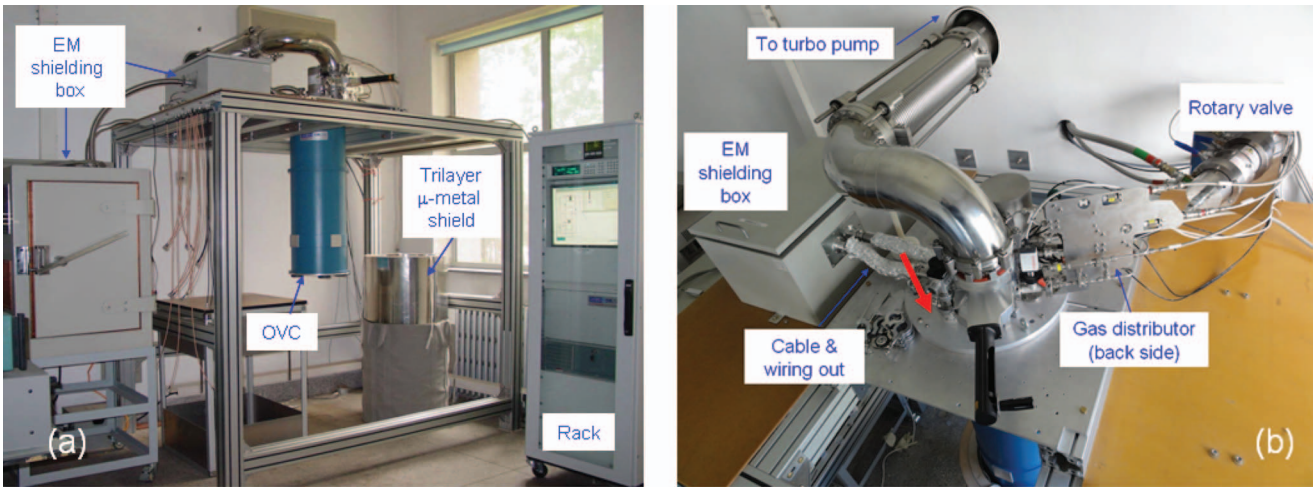

FIG. 1. Photos of the cryogen-free DR200 dilution refrigerator system suitable for qubit quantum-state measurements. (a) Front view. (b) Top view. The fridge is installed on an aluminum-alloy frame with double acoustic isolation from the ground using rubber stands and air springs. The turbo pump and rotary valve are mechanically decoupled from the fridge. The fridge is also electrically isolated from the pumps, the control instruments, and the gas lines. The thick red arrow in (b) indicates where an accelerometer sensor is placed for vibration measurement.

from the insert and securely attached to the wall, as can also be seen in Fig. 1(b). Soft plastic hoses are used for the connections to the DR unit wherever needed. Other equipments, including the forepump, the compressor (dry pump), the pulse-tube refrigerator (PTR) compressor, and a water cooler are all located in the next room. The overall arrangements of the system are schematically shown and further explained in Fig. 2.

Vibration levels of the system are measured using an accelerometer in three cases: Namely, the whole system is off, only the turbo pump is on, and both the turbo pump and the PTR are on. The results are shown in Fig. 3. The accelerometer is manufactured by Wilcoxon Research (Model 731) and its sensor is placed on the top of the refrigerator, as indicated by a thick red arrow in Fig. 1(b), which measures the vertical acceleration of the system. The sensor is connected to a preamplifier with a 450-Hz low-pass filter. The output voltage signal of the preamplifier (1 kV corresponds to 9.8 m/s^2) is then measured by a spectrum analyzer. In its power spectral density mode, we directly obtain the acceleration "power" spectral density, which has the unit $(\mathrm{m/s^2})^2/\mathrm{Hz}$, or the corresponding data presented in unit $(\mathrm{m/s^2})/\sqrt{\mathrm{Hz}}$, which we call acceleration spectral density. The velocity spectral density shown in Fig. 3 in unit $(\mathrm{m/s})/\sqrt{\mathrm{Hz}}$ are the latter data divided by ω and averaged over 400 measurements in each case.

The baseline in Fig. 3 (bottom line) decreases monotonically from 10^{-6} $(\mathrm{m/s})/\sqrt{\mathrm{Hz}}$ at low frequency (<5 Hz) to 10^{-9} $(\mathrm{m/s})/\sqrt{\mathrm{Hz}}$ at high frequency (>200 Hz), which is comparable to the data recorded in several scanning tunneling microscopy (STM) labs around the world.[5] As a result of the separation of the turbo pump from the main body of the refrigerator, we see that the velocity spectral density increases only slightly when the turbo

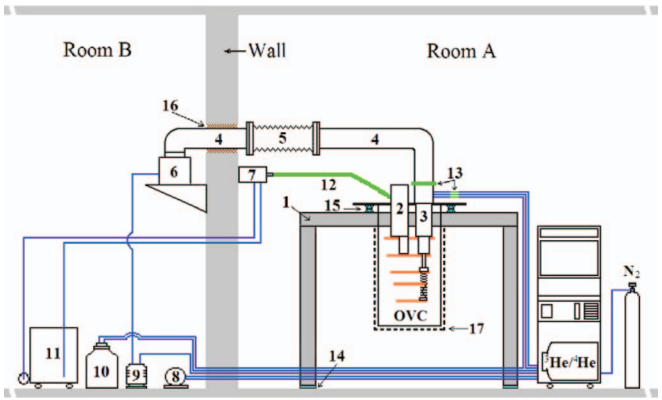

FIG. 2. Schematic overall arrangement of the cryogen-free DR200 dilution refrigerator measurement system. (1) Aluminum-alloy frame; (2) PTR cold-head; (3) and (4) pumping line; (5) bellows assembly; (6) turbo pump; (7) rotary valve; (8) compressor; (9) forepump; (10) LN2 coldtrap; (11) PTR compressor; (12) and (13) electrically isolated gas line and connecters; (14) rubber stands; (15) air-spring system (optional); (16) sand bag; (17) trilayer μ-metal shielding. Thin blue lines represent the gas lines.

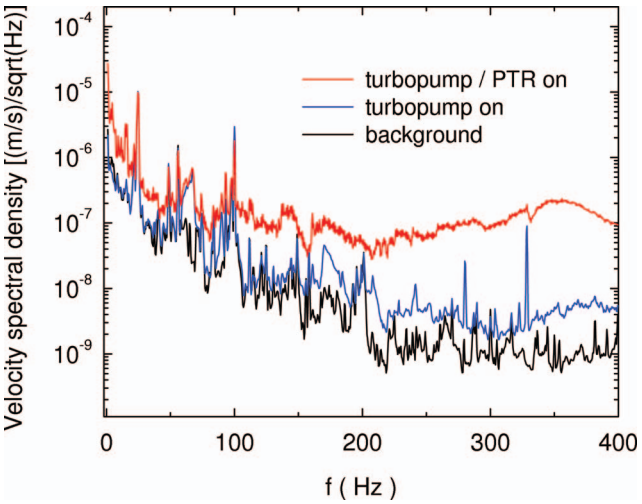

FIG. 3. Velocity spectral density of the dilution refrigerator system measured under three conditions: The whole system is off (bottom line), only the turbo pump is on (middle line), and both the turbo pump and the PTR are on (top line), respectively. See text for measurement details. Peaks at 50 Hz and its harmonics and subharmonics are due to power line interference (not due to mechanical vibrations).

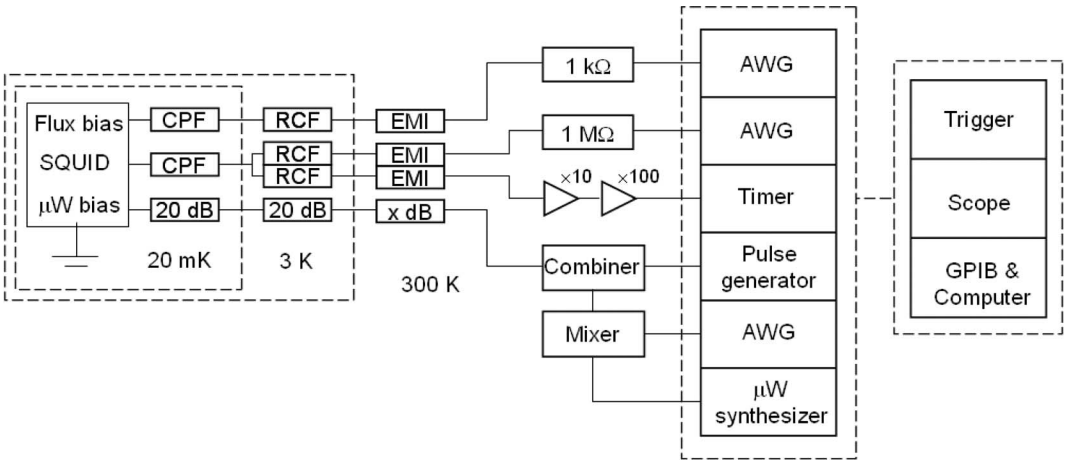

FIG. 4. Diagram of the electronic measurement system. Typical three kinds of the measurement lines are shown starting from the left side of the diagram: The qubit flux bias and SQUID-detector current lines, the SQUID-detector voltage lines, and the microwave/fast-pulse lines.

pump is switched on (middle line). On the other hand, it increases significantly, especially above about 100 Hz, when the PTR is also running (top line). This is unavoidable since the PTR is mechanically integrated to the body of the fridge. At $f > 200$ Hz, the data are approximately two orders of magnitude higher than the baseline. The results presented in Sec. IV below show that this level of vibration has negligible effect on the control and measurement of the coherent quantum dynamics of superconducting phase qubits.

III. ELECTRONIC SETUP

The electrical measurement circuit includes three types of lines: The current bias lines, the voltage sensing lines, and the microwave/fast-pulse lines, which are shown schematically in Fig. 4. The current and voltage lines from room temperature to low temperature, which are used for the qubit flux bias or superconducting quantum interference device (SQUID)-detector current bias and the SQUID-detector voltage measurement, are composed of flexible coaxial cables, electromagnetic interference (EMI) filters, resistance/capacitance (RC) filters, and copper powder filters[6,7] down to the sample platform. Flexible coaxial cables manufactured by GVL Cryoengineering with a bandwidth of dc to 300 MHz are used. The cables have ϕ 0.65 mm CuNi outer conductor, teflon dielectric, and central conductors made of ultra-low-temperature-coefficient ϕ 0.1 mm brass Ms63 (used above the 4 K plate) and of ϕ 0.1 mm superconducting NbTi (used below the 4 K plate). EMI filters placed outside the fridge at the room temperature are VLFX-470 (VLFX) low-pass filters manufactured by MiniCircuits, which are used to filtering out high frequency noises from room temperature lines. The characteristic impedance of the coaxial filter VLFX is 50 Ω and the passing band of the filter is dc to 470 MHz with attenuation greater than 40 dB between 2 and 20 GHz. RC filters are inserted into the coaxial cables and are thermally anchored to the 4 K plate. All RC filters have a 3 dB cutoff frequency of 100 kHz. To reduce joule heating R (C) is chosen to be 1 kΩ (2040 pF) and 10 kΩ (204 pF) for the current and voltage leads, respectively. The copper powder filters are made following the technique developed by Lukashenko and Ustinov.[7] Their 3 dB cutoff frequency is around 80 MHz and has more than 60 dB attenuation at 1 GHz. Their typical characteristic and final appearance of these filters are shown in Fig. 5 and the inset. These copper powder filters are mounted next to the sample platform which is at the mixing chamber temperature.

Low-noise preamplifiers are used in the voltage lines of the detector SQUIDs. These preamplifiers, with a gain of 1000, are made using two "analog devices" AD624 instrumentation amplifiers (gains set to 10 and 100, respectively) in series. The bandwidth of these preamps is 100 kHz and the noise characteristic is shown in Fig. 6. Finally, the microwave lines, shown schematically in Fig. 4, are composed of 2.2 mm diameter semirigid coaxial cables manufactured by Keycom with non-magnetic stainless steel inner/outer conductors with MiniCircuits attenuators (frequency range 0–18 GHz) to increase signal-to-noise ratio. The total attenuation coefficient in each line is typically 40 dB.

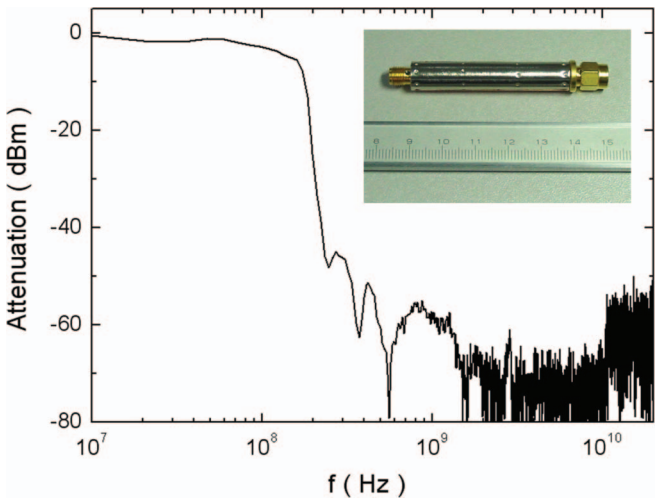

FIG. 5. Typical attenuation versus frequency characteristic of the copper powder filters. The attenuation at 120 MHz is about 3 dB, and is more than 60 dB above 1 GHz. The length of filter is 7 cm as is shown in the inset.

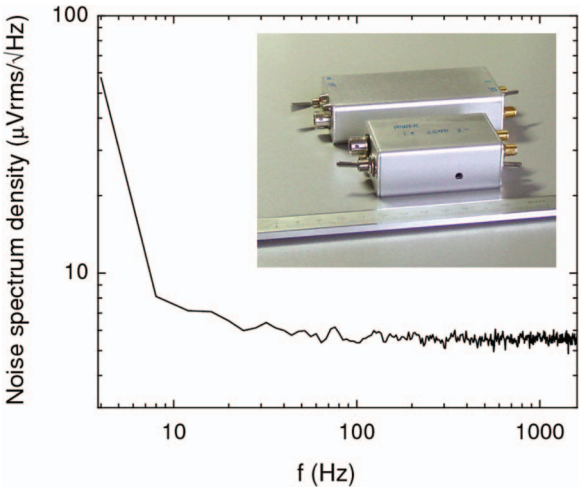

FIG. 6. Noise characteristic of a voltage preamplifier with gain of 1000 made from two AD624 instrumentation amplifiers in series. The noise spectrum density is less than 10 nV rms/$\sqrt{\text{Hz}}$ (refer to input) above ~10 Hz up to 100 kHz (flat part above 1.6 kHz not shown). The inset shows the final assembly (the longer one) together with that of an isolation amplifier with unity gain (the shorter one).

All coaxial cables and attenuators are thermally anchored to various temperature stages (namely, on the 70 K, 4 K, still, 100 mK, and mixing chamber plates). The thermal anchors for the flexible coaxial cables are made by two copper plates with a 3.5 cm section of coaxial cables clamped between them. As can be seen in Figs. 1(a) and 1(b), a smaller EM shielding box (Faraday cage) made of cold-rolled steel sheet is placed near the top of the fridge, in which EMI filters and preamplifiers are located. A trilayer μ-metal magnetic shield, also illustrated in Fig. 2, is used to reduce the ambient static field to about 20 nT. The sample holder has twelve 50 Ω coplanar waveguides (CPWs) allowing signals with frequencies up to 18 GHz to pass through with minimal reflections. The fridge is galvanically isolated from the vacuum pumps, the control instruments, and gas lines so that the system can be electrically connected to a dedicated ground post. We also use an optical coupler in the control line to achieve galvanic isolation between the refrigerator and the control rack (see Fig. 1). Our tests showed that this setup is adequate for measuring coherent quantum dynamics of Josephson qubit circuits as described in detail below.

IV. QUANTUM COHERENT-STATE MEASUREMENTS

In order to qualify our system for qubit experiments, we chose to measure coherent dynamics of a superconducting phase qubit, which is extremely sensitive to its EM environment. As an initial characterization of the electronic system, we measured the switching current distribution $P(I)$ of a Nb dc-SQUID with the loop inductance much smaller than the Josephson inductance of the junctions so that the SQUID behaves as a single junction with critical current I_c tunable by applying a magnetic field.[8] From the measured width σ of $P(I)$ versus temperature, we found that σ continuously decrease to as low as 4 nA at 20 mK by reducing I_c and as low as 1 nA near 1 K due to phase diffusion[9,10] indicating a current noise level below 1 nA in our measurement circuit.

The flux biased phase qubit had similar layout and parameters as that described in Ref. 11 and was coupled to an asymmetric dc-SQUID to readout its quantum state. A current bias line was used to apply an external magnetic flux to the qubit loop which controls the shape of the potential energy landscape and the level separation E_{10} between the ground and first excited states of the qubit. For a given E_{10}, a short resonant microwave pulse of variable length with frequency $f_{10} = E_{10}/h$ was applied, which coherently transfers population between the ground state and the first excited state. Consequently, we observed Rabi oscillations by keeping the amplitude of the microwave field constant while varying the duration of the modulation pulses. Data obtained with microwave frequency of about 16 GHz are shown in Fig. 7(a) as symbols. A simple fit to an exponentially damped sinusoidal function yields a decay time of 70 ns. In Fig. 7(b), the Rabi frequency versus microwave amplitude, which shows the expected linear dependence, is displayed.

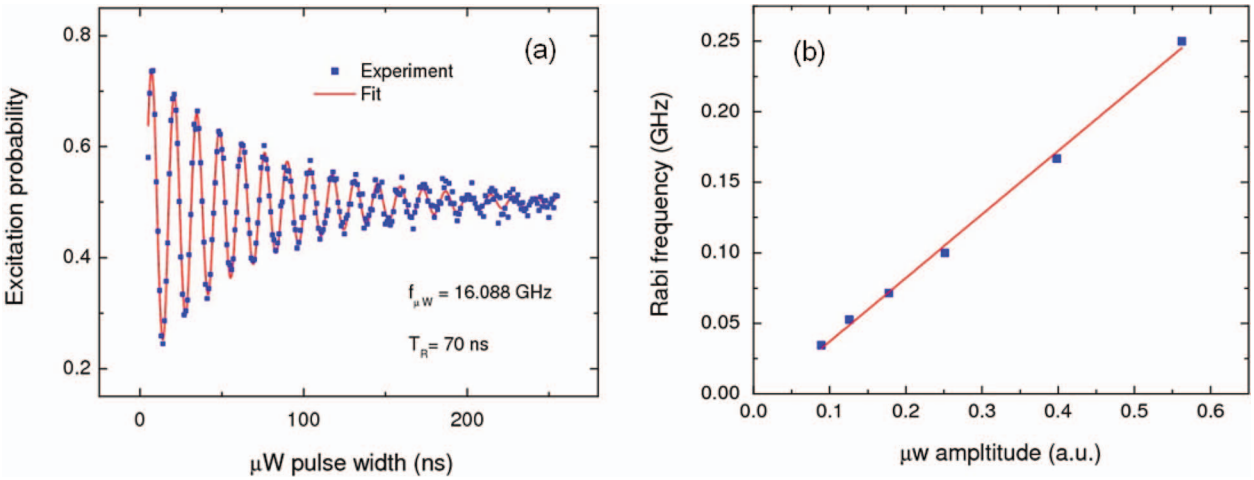

FIG. 7. (a) Rabi oscillation measured from an rf-SQUID type phase qubit made of Al Josephson junction (symbols). The applied microwave frequency is ~16 GHz and a decay time of 70 ns is obtained from the exponentially damped sinusoidal oscillation fit (line). (b) Rabi frequency versus microwave amplitude (symbols). The line is a guide to the eye.

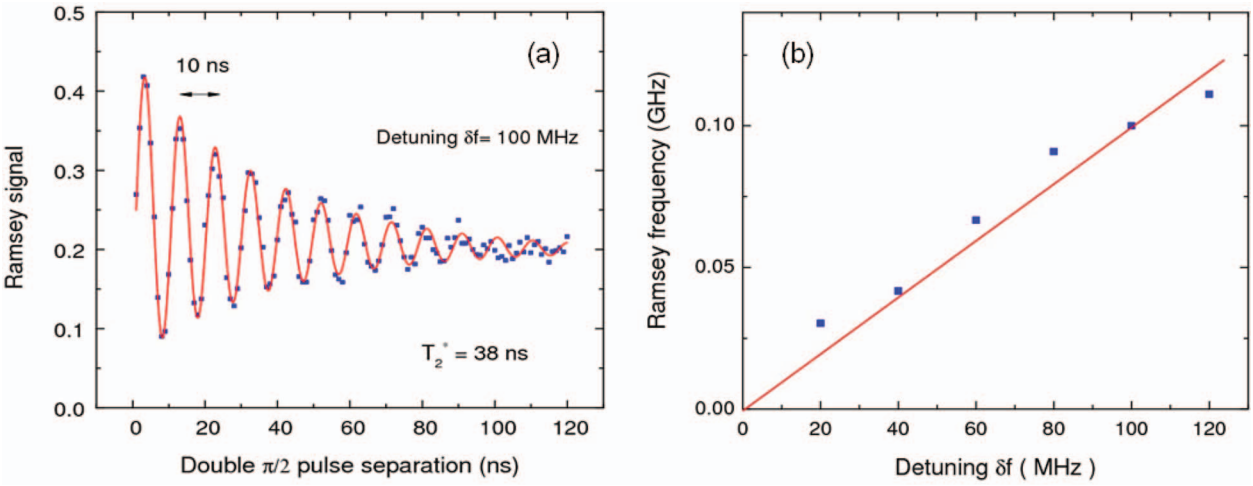

FIG. 8. (a) Ramsey fringe measured from an rf-SQUID type phase qubit made of Al Josephson junction (symbols). The applied microwave frequency is ~16 GHz and a decay time of 38 ns is obtained from the exponentially damped sinusoidal oscillation fit (line). (b) Ramsey frequency versus detuning (symbols). The line is a guide to the eye.

Ramsey interference was also observed in the phase qubit by applying two $\pi/2$ pulses, separated by a time delay τ. Manipulation of the qubit state for Ramsey pulse sequence can be explained in terms of the Bloch sphere and Bloch vectors.[3] The first $\pi/2$ pulse rotates the qubit state vector to the x-y plane, where it is allowed to evolve around the z axis freely for a duration of τ. Subsequently, the second $\pi/2$ pulse is applied which is followed immediately by qubit state readout. When the microwave frequency is detuned slightly by a mount δf away from f_{10}, the final state of the qubit at the end of the second $\pi/2$ pulse will be a superposition of the ground (the first excited) state with probability amplitude $\cos 2\pi\delta f\tau$ ($\sin 2\pi\delta f\tau$). The sinusoidal dependence of the state probabilities on time can then be obtained by varying τ. Figure 8(a) shows the measured Ramsey fringe with a period of $1/\delta f$ for $\delta f = 100$ MHz. Fitting the data to exponentially damped sinusoidal oscillation leads to a decay (dephasing) time of $T_2^* = 38$ ns. The linear dependence of the Ramsey frequency on detuning can be seen in Fig. 8(b).

These results are comparable to those obtained from the same phase qubit using a qubit-experiment-qualified wet dilution refrigerator and thus clearly demonstrate that our cryogen-free dilution refrigerator provides a good low-temperature, low-noise platform for delicate experiments such as measuring the coherent quantum dynamics of Josephson phase qubit described above. What is worthy to mention is that the overall design and construction of our system, built in a laboratory which is not electromagnetically shielded, are relatively easy to achieve with minimal additional cost. The realization of the present system should be useful also for the quantum-state measurements at low temperatures of many other physical systems whose properties and dynamics are very sensitive to fluctuations in their environment.

ACKNOWLEDGMENTS

We are grateful to Junyun Li of Oxford Instruments Shanghai Office for his continuous support in this work and to H. J. Gao, L. Shan, and C. Ren for their kind help during vibration measurements. The work at the Institute of Physics was supported by the National Natural Science Foundation of China (Grant Nos. 10874231 and 11104340) and the Ministry of Science and Technology of China (Grant Nos. 2009CB929102 and 2011CBA00106).

[1] Y. Makhlin, G. Schön, and A. Shnirman, Rev. Mod. Phys. **73**, 357 (2001).
[2] A. Wallraff, A. Lukashenko, C. Coqui, A. Kemp, T. Duty, and A. V. Ustinov, Rev. Sci. Instrum. **74**, 3740 (2003).
[3] J. Clarke and F. K. Wilhelm, Nature (London) **453**, 1031 (2008).
[4] J. Q. You and F. Nori, Nature (London) **474**, 589 (2011).
[5] J. E. Hoffman, Ph.D. dissertation, University of California, Berkeley, 2003).
[6] J. M. Martinis, M. H. Devoret, and J. Clarke, Phys. Rev. B **35**, 4682 (1987).
[7] A. Lukashenko and A. V. Ustinov, Rev. Sci. Instrum. **79**, 014701 (2008).
[8] H. F. Yu, X. B. Zhu, Z. H. Peng, W. H. Cao, D. J. Cui, Y. Tian, G. H. Chen, D. N. Zheng, X. N. Jing, Li Lu, S. P. Zhao, and S. Y. Han, Phys. Rev. B **81**, 144518 (2010).
[9] S.-X. Li, W. Qiu, S. Han, Y. F. Wei, X. B. Zhu, C. Z. Gu, S. P. Zhao, and H. B. Wang, Phys. Rev. Lett. **99**, 037002 (2007).
[10] H. F. Yu, X. B. Zhu, Z. H. Peng, Y. Tian, D. J. Cui, G. H. Chen, D. N. Zheng, X. N. Jing, Li Lu, S. P. Zhao, and S. Han, Phys. Rev. Lett. **107**, 067004 (2011).
[11] M. Neeley, R. C. Bialczak, M. Lenander, E. Lucero, M. Mariantoni, A. D. O'Connell, D. Sank, H. Wang, M. Weides, J. Wenner, Y. Yin, T. Yamamoto, A. N. Cleland, and J. M. Martinis, Nature (London) **467**, 570 (2010).